

## Non-Gaussian limit fluctuations in active swimmer suspensions

Takashi Kurihara,<sup>1</sup> Msato Aridome,<sup>1</sup> Heev Ayade,<sup>1</sup> Irwin Zaid,<sup>2</sup> and Daisuke Mizuno<sup>1,\*</sup>

<sup>1</sup>*Kyushu University, Fukuoka 812-8581, Japan*

<sup>2</sup>*Rudolf Peierls Center for Theoretical Physics, University of Oxford, Oxford OX1 3NP, United Kingdom*

(Received 8 June 2016; revised manuscript received 18 January 2017; published 9 March 2017)

We investigate the hydrodynamic fluctuations in suspensions of swimming microorganisms (*Chlamydomonas*) by observing the probe particles dispersed in the media. Short-term fluctuations of probe particles were superdiffusive and displayed heavily tailed non-Gaussian distributions. The analytical theory that explains the observed distribution was derived by summing the power-law-decaying hydrodynamic interactions from spatially distributed field sources (here, swimming microorganisms). The summing procedure, which we refer to as the physical limit operation, is applicable to a variety of physical fluctuations to which the classical central limiting theory does not apply. Extending the analytical formula to compare to experiments in active swimmer suspensions, we show that the non-Gaussian shape of the observed distribution obeys the analytic theory concomitantly with independently determined parameters such as the strength of force generations and the concentration of *Chlamydomonas*. Time evolution of the distributions collapsed to a single master curve, except for their extreme tails, for which our theory presents a qualitative explanation. Investigations thereof and the complete agreement with theoretical predictions revealed broad applicability of the formula to dispersions of active sources of fluctuations.

DOI: [10.1103/PhysRevE.95.030601](https://doi.org/10.1103/PhysRevE.95.030601)

### I. INTRODUCTION

Properties of small systems fluctuate measurably and statistics of such fluctuations are often the key to investigate their physical behaviors [1,2]. In a homogeneous continuum under thermodynamic equilibrium, for instance, a micron-sized probe particle exhibits Brownian motion due to incessant independent collisions of innumerable molecules. The variance of the local stress attributable to these collisions is finite and quantitatively related to the continuum mechanics of surrounding media via the fluctuation-dissipation theorem [3]. The classical central limit theorem (CLT) guarantees that the sum of independent fluctuations with finite variance converges to Gaussian. Thermal probe fluctuations in homogeneous continuum are therefore Gaussian, which is a stable distribution for variables whose variance is finite [4].

Phenomena at the mesoscopic scales are more than just stochastic. Sometimes they are even chaotic as typically observed in an active material [5,6]; i.e., a system driven out of equilibrium by force-generating inclusions such as microorganisms swimming in buffer [7–9], or motor proteins in cytoskeletons [10–12]. These active materials exhibit peculiar rheological properties and collective behaviors that do not obey the statistics of thermodynamic equilibrium [11,13]. For their theoretical description, coarse graining, i.e., taking quantities such as the concentration, orientation, and flows as continuum fields [8,9], has been adopted. Formally, it can be validated for systems concentrated with active inclusions. Frequently, however, active force generators such as microorganisms and motor proteins are sparsely distributed in space. Their average nearest-neighbor distance can be much larger than the probe size. Fluctuations are thus collective and correlated at least in the distance of active inclusions. Such fluctuations have been studied with numerical simulations

[14] and/or phenomenological modeling [15]. Criterion for the applicability of the CLT to fluctuations in active suspensions or to other general physical systems is still elusive.

A suspension of swimming microorganisms has been used as a simple model of an active material [7–9,13]. Microorganisms can swim since they create forces and transmit them to the surrounding media. For instance, *Chlamydomonas reinhardtii*, which was chosen for this study, pulls on the surrounding fluid using two flagella at its front to move its body forward (Fig. 1). The resulting flows in the surrounding media were studied by tracking the motion of colloidal probe particles. It has been found that displacements of the probe particles show non-Gaussian heavily tailed distributions [16,17]. In a whole sample with macroscopic dimensions, many *Chlamydomonas* independently swim and generate forces. If the flow generated by a *Chlamydomonas* has finite variance, CLT requires that probe fluctuations that arise as the sum of independent flows from many *Chlamydomonas* should converge to Gaussian distribution. The observed non-Gaussianity seems to apparently violate CLT.

The hydrodynamic flow field around a force generator (*Chlamydomonas*) spatially decays with a power-law function. It is then possible to show that the field intensity due to a single *Chlamydomonas* that is randomly placed in the system should exhibit power-law distribution. If such power-law distribution was attained in an infinite range, its variance would diverge. The generalized central limit theorem (G-CLT) would then require that sum flow field should converge to another limit distribution referred to as Lévy stable distribution [4,18]. However, the variance of the physical power-law fields does not diverge since they are usually truncated at its larger end somehow. In the case of *Chlamydomonas* suspension, infinitely large fluctuation does not occur since a probe and a force generator do not share the same position. Therefore, G-CLT does not explain the observed non-Gaussianity.

Both the classical CLT and G-CLT are broken in active swimmer suspension, since the standard limit operation

\*Corresponding author: [mizuno@phys.kyushu-u.ac.jp](mailto:mizuno@phys.kyushu-u.ac.jp)

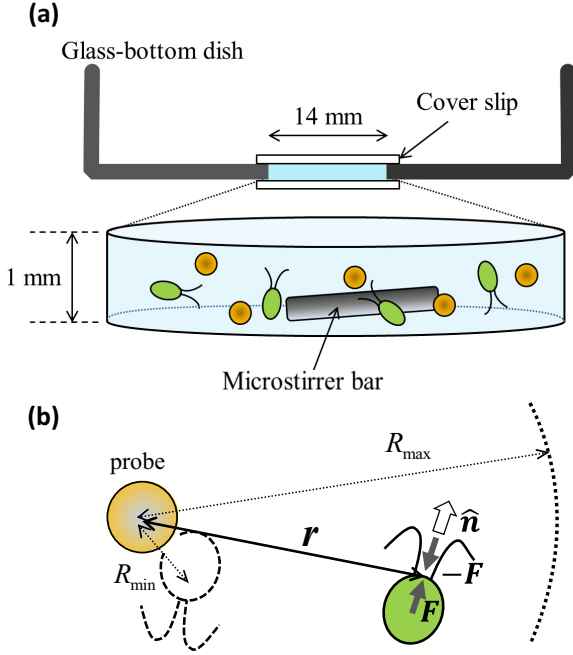


FIG. 1. (a) *Chlamydomonas* were dispersed and sealed in a glass-bottom dish together with microstirrer bars. (b) A single *Chlamydomonas* was randomly inserted into a spherical volume, and a probe was placed at the origin. A pair of balanced forces  $\mathbf{F}$  and  $-\mathbf{F}$  were exerted on the surrounding medium and form a force dipole. The swimming direction is represented by  $\hat{\mathbf{n}}$ .

adopted for these conventional CLT cannot be used for summing hydrodynamic power-law fields. As we show below, the limit distribution of the fluctuations induced by all *Chlamydomonas* in the macroscopic sample is attained, not by just increasing the *Chlamydomonas* number in the system, but by taking the infinite system size while keeping the concentrations of *Chlamydomonas* constant. This “physical” limit operation increasing the system size affects the distribution of the flow originated from a single *Chlamydomonas*; the power-law range of the distribution extends towards smaller values during the operation. As was found recently, the limit operation appropriate for physical situation leads to an analytical formula that smoothly intermediates the mathematical limit distributions, Gauss and Lévy [19]. Below, we first summarize its derivation and extend the formula so that it can compare to experimental observations of hydrodynamic fluctuations in active swimmer suspensions.

## II. THEORETICAL BASIS

Lévy distribution is defined by its Fourier transform (characteristic function) in the form of  $\tilde{P}(k) = \exp(-b|k|^\alpha)$  where the characteristic exponent  $\alpha$  is restricted to  $0 < \alpha < 2$ . Suppose that there are  $N$ -independent *Chlamydomonas* swimming in a spherical volume with a radius  $R_{\max}$ . A probe particle is placed at its center, which is defined as the origin of the system (Fig. 1). In dilute situations, each *Chlamydomonas* independently swims and contributes to the velocity of the probe as  $\mathbf{v}_1, \mathbf{v}_2, \mathbf{v}_3, \dots, \mathbf{v}_N$ . The probability distribution  $W(\mathbf{v})$  of the total velocity  $\mathbf{v} = \sum_{i=1}^N \mathbf{v}_i$  is then given by the  $(N-1)$ -

fold convolution of  $w_i(\mathbf{v}_i)$  which is the probability distribution of  $\mathbf{v}_i$ . In Fourier space, the characteristic function of  $W(\mathbf{v})$  is expressed as

$$\tilde{W}(k) = \prod_i \tilde{w}_i(k). \quad (1)$$

Hereafter, the use of “ $\sim$ ” above a function indicates that it has undergone Fourier transform. Consider now that all  $w_i(\mathbf{v}_i)$  are isotropic and take the same probability distribution, i.e.,  $w(v_i) \equiv w_i(\mathbf{v}_i)$  where  $v_i \equiv |\mathbf{v}_i|$ . When  $w(v)$  exhibits a heavy tail that follows a power law  $\sim 1/v_i^{3+\alpha}$ , its variance diverges when  $\alpha$  is in the range  $0 < \alpha < 2$ . In this case, according to the G-CLT that is extended for stochastic variables with infinite variance,  $W(v) \equiv W(\mathbf{v})$  converges to Lévy stable distributions [4,19,20].

Swimming microorganisms have been modeled as force dipoles as a first approximation [21]. Because of the mesoscopic size of the microorganisms, low Reynolds number hydrodynamics is relevant. Since inertia is neglected, flows in the media instantaneously respond to the applied forces [22,23]; the pulling thrust applied by the flagella must be counterbalanced with the drag of surrounding fluid over the body. There is no monopole contribution because of the force balance. The effects of higher-order multipoles are not negligible if it is too close to the *Chlamydomonas* [24,25]. However, they decay much quicker away from the force generators. Regardless of the perturbation of the flows close to a *Chlamydomonas*, overall velocity fields precisely follow  $v(\hat{\mathbf{n}}, \mathbf{r}) \propto 1/r$  in two-dimensional (2D) suspensions [25] and approximately follow  $v(\hat{\mathbf{n}}, \mathbf{r}) \propto 1/r^2$  in three-dimensional (3D) suspensions [24,26]; both are consistent to the force-dipole model. Note that 2D particle tracking can be performed with more precision compared to 3D experiments, and  $v(\hat{\mathbf{n}}, \mathbf{r}) \propto 1/r$  in 2D supports  $v(\hat{\mathbf{n}}, \mathbf{r}) \propto 1/r^2$  in 3D.

Suppose that the  $i$ th *Chlamydomonas* is placed at  $\mathbf{r}$  with orientation  $\hat{\mathbf{n}}$  and strength  $\kappa$  (Fig. 1). The velocity of the flow at the origin is then given by

$$\mathbf{v}_i(\hat{\mathbf{n}}, \mathbf{r}) = \kappa \{3(\hat{\mathbf{r}} \cdot \hat{\mathbf{n}})^2 - 1\} \hat{\mathbf{r}} / 8\pi\eta r^2 \equiv \boldsymbol{\gamma} / r^2 \quad (2)$$

up to the lowest order of  $1/r$  [27]. Here,  $\hat{\mathbf{r}} \equiv \mathbf{r}/r$ ,  $\eta$  is the viscosity of the fluid, and  $\boldsymbol{\gamma}$  represents the direction and strength ( $\gamma \sim \kappa/8\pi\eta$ ) of the induced flow. Next, suppose that we put a single *Chlamydomonas* in random orientations and positions in an infinite spherical volume ( $R_{\max} \rightarrow \infty$ ). Taking  $\mathbf{r}$  and  $\hat{\mathbf{n}}$  as random vector variables, the isotropic power-law distribution of the velocity is obtained:  $w(v_i) \equiv w(\mathbf{v}_i) \propto v_i^{-9/2}$ , meaning  $\alpha = 3/2$  [28,29]. If this power-law distribution was obtained in an infinite range, its variance diverges. If we take the simple mathematical sum of these fluctuations,  $W(\mathbf{v}) \equiv W(\mathbf{v})$  should converge to the Lévy stable distribution with the same power-law tail  $\propto v^{-9/2}$  [4,18–20].

The unphysical divergence of the variance arises because the model neglects the finite sizes of objects, such as the *Chlamydomonas* and the probe. As shown in Fig. 1, there is minimum distance  $R_{\min}$  between a probe and a *Chlamydomonas*. In this case,  $w(v_i)$  follows the power law  $\sim 1/v_i^{9/2}$  in a range  $v_{\min} \equiv \gamma_{\min}/R_{\max}^2 < v_i < v_{\max} \equiv \gamma_{\max}/R_{\min}^2$  but it is truncated outside.  $w(v_i)$  is therefore approximated with a

power-law function truncated at  $v_{\min}$  and  $v_{\max}$  as

$$w(v) = \begin{cases} \frac{\alpha v_{\min}^\alpha}{4\pi} v^{-(3+\alpha)} \left[1 - \left(\frac{v_{\min}}{v_{\max}}\right)^\alpha\right]^{-1} & (v_{\min} < v < v_{\max}) \\ 0 & (\text{otherwise}). \end{cases} \quad (3)$$

Whereas the actual flow around a force dipole is anisotropic and  $\gamma$  might distribute, they merely obscure the truncation. Based on the analysis including  $\hat{n}$  dependence of  $v_i$ , we estimate  $\gamma_{\min} \lesssim \gamma$  and  $\gamma < \gamma_{\max} < 2\gamma$  [19]. Substituting the Fourier transform of Eq. (3) in Eq. (1), and by taking the limit of a large system size ( $R_{\max} \rightarrow \infty$ ,  $N \rightarrow \infty$ ) with  $N(v_{\min}/v_{\max})^{3/2} = \beta c R_{\min}^3$  being constant, the limit distribution is obtained [19]:

$$\tilde{W}(k_v) = \exp\left(\beta c R_{\min}^3 \left[1 - {}_1F_2\left(-\frac{3}{4}; \frac{3}{2}, \frac{1}{4}; -\frac{\gamma_{\max}^2 k_v^2}{4R_{\min}^4}\right)\right]\right). \quad (4)$$

Here,  ${}_1F_2$  denotes the hypergeometric function and  $c$  is the number density of the *Chlamydomonas*.  $\beta \equiv 4\pi/3(\gamma_{\min}/\gamma_{\max})^{3/2}$  is a prefactor with the order of unity that is removed hereafter. It is to be noted that  $v_{\min}$  approaches zero during this limit operation. This leads to a continuous increase in the range of power-law distribution, whereas its variance becomes infinitesimally small. This subtle balance leads to nonstandard physical limit distributions. Provided that the *Chlamydomonas* suspension is isotropic, the flow velocity distribution in the  $x$  direction is obtained by the one-dimensional Fourier transform,  $W(v_x) = \frac{1}{2\pi} \int_{-\infty}^{\infty} \tilde{W}(k_{vx}) e^{-ik_{vx}v_x} dk_{vx}$ .

The crucial quantity that determines the distribution given in Eq. (4) is  $\Phi \equiv cR_{\min}^3$ . In Fig. 2(a),  $\sigma W(v_x)$  is plotted versus  $v_x/\sigma$  for various  $c$ ,  $R_{\min}$ , and fixed  $\gamma = 1.5 \times 10^{-15}$  [m<sup>3</sup>/s].  $\sigma^2 = -\partial^2 \tilde{W}(k_{vx})/\partial k_{vx}^2|_{k_{vx}=0} = c\gamma^2/R_{\min}$  is the variance of  $W(v_x)$ .  $\gamma$  was arbitrarily chosen since the rescaled plot does not depend on it. The normalized distributions with the same  $\Phi$  are plotted in the same colors and clearly demonstrate the collapse to a single curve. When  $\Phi$  is small, the distributions are heavily tailed and asymptotically approach a Lévy distribution that should exhibit power-law tail  $\propto v_x^{-5/2}$  [broken curve in Fig. 2(a)]. Note that this power law corresponds to  $\propto v^{-9/2}$ . When  $\Phi$  is large, they converge to Gaussian [dash-dotted curve in Fig. 2(a)]. The distributions are scaled solely with  $\Phi$  that indicates the number of *Chlamydomonas* in the spherical volume with radius  $R_{\min}$ , as schematically shown in Fig. 2(b).

### III. METHODS

Experiments were carried out using the strain *Chlamydomonas reinhardtii* (NIES collection, NIES-2236). *Chlamydomonas* were cultured in distilled water containing 0.5% Hyponex (Hyponex Japan Corp.) under the illumination of a fluorescent lamp. The suspensions of *Chlamydomonas* were concentrated by centrifugation at 7500 rpm (5000  $\times g$ ) and then resuspended in the glass-bottom dish (D11130H, Matsumi Glass Ind.) together with fluorescent probe particles (Magsphere Inc., diameters 5 and 10  $\mu\text{m}$ ) and microstirrers (VP717-1, V&P Scientific). The dish has a 14-mm-diameter hole at the bottom that is covered by a laminated No. 1 coverslip. This circular region was filled with suspension to a

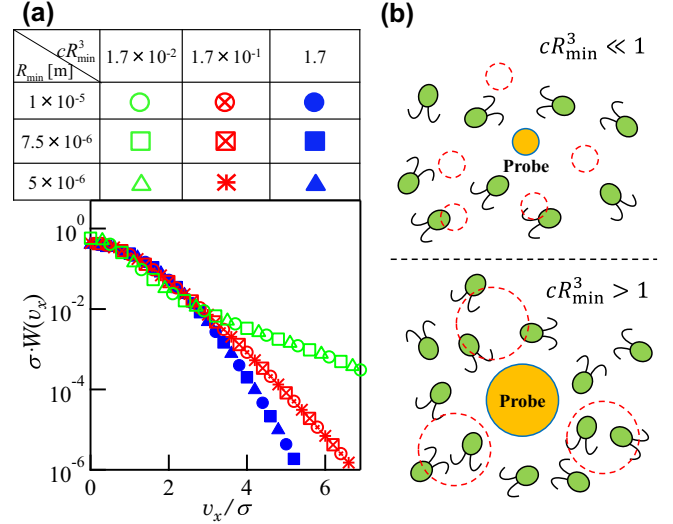


FIG. 2. (a) Theoretical curves of normalized  $W(v_x)$  versus  $v_x/\sigma$ . Plots with the same  $cR_{\min}^3$  are shown in the same color and collapse to the same curve. The predicted curves for  $cR_{\min}^3 \ll 1$  approach a heavily tailed Lévy distribution that is characterized with its power-law tail  $\propto v_x^{-5/2}$  (broken curve), whereas those corresponding to  $cR_{\min}^3 \gg 1$  converge to Gaussian distributions (dash-dotted curve). (b) Schematic illustration of  $cR_{\min}^3$  that indicates the numbers of *Chlamydomonas* in the  $R_{\min}^3$  volumes, which are indicated by the dashed circles.

full depth of 1 mm, and an airtight seal was made by another No. 1 coverslip over the region (Fig. 1). Probe particles were observed mid-height in the chamber to avoid surface effects. Inhomogeneities of *Chlamydomonas* and their adherence to the glass surface were negligible since the measurements were done after stirring the suspension with microstirrers. The number density of *Chlamydomonas* was obtained for each experiment by counting the population using hemacytometers (Thoma). Fluorescently labeled polystyrene latex particles were tracked under a fluorescence microscope (TU-2000, Nikon). Fluorescence images were captured with a NI-IMAQ 1408 board (National Instruments) at the video rate (30 Hz) and the positions of fluorescence particles were obtained with custom-made LABVIEW software.

### IV. RESULTS AND DISCUSSIONS

In the dilute conditions chosen in this study ( $2.7 \times 10^{12} \text{ m}^{-3} < c < 3.6 \times 10^{13} \text{ m}^{-3}$ ), the swimming behavior of different *Chlamydomonas* is hardly correlated. They swim at similar speeds [ $\sim 80 \mu\text{m/s}$ , Fig. 3(a)], and turn their swimming directions at intervals longer than 10 s, on average [16]. In the smallest time intervals attainable ( $\Delta t = 1/30$  s), the distance traveled by a *Chlamydomonas* is smaller than  $R_{\min}$ . Consequently, the flow variation at the probe during  $\Delta t = 1/30$  s is not large. Taking this into account, we assume that the flow at the origin purely due to the swimming of *Chlamydomonas* does not change much. The Fourier transform of nonthermal probe displacements is therefore given by  $\tilde{F}_{\text{Ch}}(k; \Delta t) = \tilde{W}(k\Delta t)$ . Finally, the short-lag-time in-plane

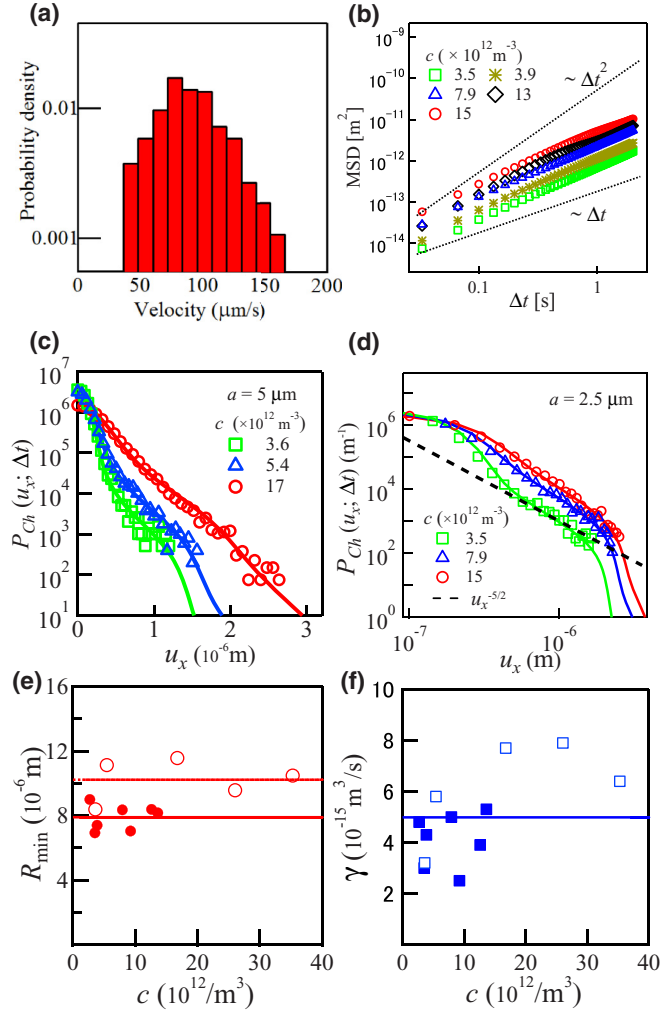


FIG. 3. (a) Velocity distribution of *Chlamydomonas*. (b) MSD of probes ( $2a = 5 \mu\text{m}$ ) in *Chlamydomonas* suspensions. Superdiffusive motion at small  $\Delta t$  tends to become diffusive ( $\text{MSD} \propto \Delta t$ ) at longer time periods. (c), (d) Displacement distributions of probes [ $2a = 10$  and  $5 \mu\text{m}$  for (c) and (d), respectively] in *Chlamydomonas* suspensions prepared with different number densities  $c$ . The curves are fits of the inverse Fourier transform in Eq. (3) obtained using  $R_{\min}$  and  $\gamma$  as fit parameters. The broken line is the power law  $\propto u_x^{-5/2}$  expected for the corresponding Lévy distribution. (e), (f) Fit values for  $R_{\min}$  and  $\gamma$ . Open and filled symbols correspond to data for probes with  $2a = 10$  and  $5 \mu\text{m}$ , respectively. Solid and dashed lines in (e) indicate the averages for probes with  $2a = 10$  and  $5 \mu\text{m}$  that exactly match to the sum of the probe radius and that of *Chlamydomonas* ( $\sim 5 \mu\text{m}$ ). The solid line in (f) indicates the average of  $\gamma$  that agrees with independent estimation [30].

displacement distribution can be written as

$$\tilde{P}_{\text{Ch}}(k_x; \Delta t) = \exp \left[ c R_{\min}^3 \left\{ 1 - {}_1F_2 \left( -\frac{3}{4}; \frac{3}{2}, \frac{1}{4}; -\frac{\gamma^2 k_x^2 \phi(\Delta t)}{4 R_{\min}^4} \right) \right\} - D k_x^2 \Delta t \right]. \quad (5)$$

The last term in the exponent in Eq. (5) indicates the additional probe fluctuation due to thermal diffusion. The diffusion

coefficient  $D$  was estimated in this study by observing the Brownian motion of the same probe particles after removing the *Chlamydomonas* via centrifugation. Obviously, we choose  $\phi(\Delta t) = \Delta t^2$  for small  $\Delta t$  ( $= 1/30$  s) since we expect that nonthermal motion of a probe is ballistic. But it can evolve differently in longer time scales since temporal fluctuation of the hydrodynamic flow affects probe displacements.

Figure 3(b) shows the mean square displacements [ $\text{MSD}(\Delta t) \equiv \langle \{u_x(t + \Delta t) - u_x(t)\}^2 \rangle$ ] of probes ( $2a = 5 \mu\text{m}$ ) dispersed in *Chlamydomonas* suspensions. It was reported that MSD in *Chlamydomonas* suspensions evolves linearly with  $\Delta t$  similar to thermal diffusion [16]. We reasonably observed similar behavior only at large  $\Delta t$  ( $\geq 1$  s). At smaller  $\Delta t$ , we observed clear superdiffusive behavior [ $\text{MSD}(\Delta t) \propto \Delta t^{1.5}$ ], which is consistent with our theoretical modeling. The more ballistic probe motion expected for short-term behavior  $\text{MSD}(\Delta t) \propto \Delta t^2$  is possibly obscured by thermal fluctuations. Because of the fluctuations of flows induced by *Chlamydomonas*, probe movement loses its memory and becomes Markov ( $\text{MSD} \propto \Delta t$ ) at longer time scales. Figures 3(c) and 3(d) present typical  $P_{\text{Ch}}(u_x; \Delta t)$  measured at  $\Delta t = 1/30$  s using probes with radii  $a = 5$  and  $2.5 \mu\text{m}$ , respectively. The curves are the fits of the inverse Fourier transform of Eq. (3), and they agree well with the experimental data. The dashed line in Fig. 3(d) indicates the power law  $\propto u_x^{-1-3/2}$  consistent for Lévy distribution that is expected asymptotically for small  $\Phi$ . The symbols in Figs. 3(e) and 3(f) indicate the values of  $R_{\min}$  and  $\gamma$ , respectively, that were obtained for samples prepared with different concentrations and probe sizes. The dashed and solid lines in Fig. 3(e) indicate the averaged  $R_{\min}$  for  $a = 5$  and  $2.5 \mu\text{m}$ , respectively. The value of  $R_{\min}$  obtained by the fit is reasonable since it is consistent with the sum of the radii of the probe and *Chlamydomonas* ( $\sim 5 \mu\text{m}$ ). The force generated by each swimming *Chlamydomonas* in an aqueous medium is  $\sim 30$  pN [29]. By estimating the separation of monopoles constituting the force dipole of each *Chlamydomonas* to be equal to its radius ( $\sim 5 \mu\text{m}$ ), the magnitude of the force dipole,  $\kappa$ , was estimated to be  $\sim 1.5 \times 10^{-16}$  Nm.  $\gamma$  was then obtained using  $\gamma \sim \kappa/8\pi\eta \sim 5 \times 10^{-15}$  m<sup>3</sup>/s; this value is also consistent with the average of our fit results as shown by the solid line in Fig. 3(f).

We now discuss the time evolution of  $P_{\text{Ch}}(u_x; \Delta t)$  using the plot normalized to  $u_x/\sigma$ , which is shown in Fig. 4(a). With this rescaling, our data taken at different lag times ( $1/30 \text{ s} \leq \Delta t \leq 1$  s) collapsed to a single master curve [16]. Each second, each *Chlamydomonas* moves  $\sim 80 \mu\text{m}$ , which is much larger than  $R_{\min}$ . The flow velocity at the probe can thus change during  $\Delta t$  if there is a *Chlamydomonas* nearby [Fig. 4(c), right]. Under the dilute conditions investigated in this study ( $\Phi \equiv c R_{\min}^3 \sim 10^{-2}$ ), it is rare to have a single *Chlamydomonas* close to the probe. Then it takes more time to alter the flow velocity at the probe [Fig. 4(c), left]; these *Chlamydomonas* arrangements are prevalent and contribute to the relatively small probe displacements that show universal collapse.

By closely examining Fig. 4(a), it is seen that only the central parts ( $|u_x/\sigma| < 5$ ) of the normalized distributions overlap. The extreme tails outside this range did not collapse since they were mostly caused by *Chlamydomonas* that coincidentally passed near the probe. In this case, the local field near the *Chlamydomonas* is not represented by Eq. (2)

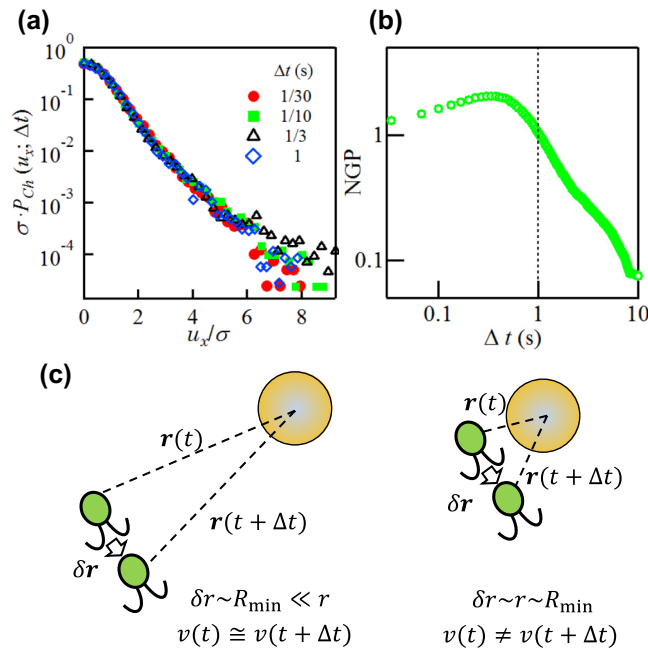


FIG. 4. (a) The lag-time dependence of  $P_{Ch}(u_x; \Delta t)$ , which was normalized by  $\sigma$ , for  $c = 1.7 \times 10^{13} \text{ m}^{-3}$  and a probe diameter of 10  $\mu\text{m}$ . For these data which have  $\Delta t \leq 1$  s, the central part of each distribution in the range  $|u_x/\sigma| < 5$  has collapsed onto a single curve. (b) Time evolution of the NGP calculated from the same data used in (a). (c) When there are no *Chlamydomonas* close to the probe (left), the complex flow close to a *Chlamydomonas* is mostly negligible. A single *Chlamydomonas* appearing by chance close to a probe (right) causes large, unpredictable displacements. These displacements affect the extreme tails of the distributions and are rarely observable with sufficient statistics.

[24,25]. A large deviation of the probe from the origin can also compromise our theory. As  $\Delta t$  increases, the probability of a *Chlamydomonas* passing near the probe also increases. The displacement fluctuations of probes observed at longer lag times ( $\Delta t > 1$  s) thus tend to converge to Gaussian distributions [31]. This trend is evident in Fig. 4(b) where the non-Gaussian parameter (NGP [32]) becomes negligible

at  $\Delta t > 1$  s. During such long lag times, a *Chlamydomonas* moves more than the average distance between neighboring *Chlamydomonas* (70–100  $\mu\text{m}$ ); the memory of the original *Chlamydomonas* arrangement was completely lost and the fluctuations of the probe particles were randomized. Classical CLT can then be applied to fluctuations at longer  $\Delta t$  since they can be described as the sum of independent random displacements in smaller time periods.

## V. CONCLUSIONS

We observed nonthermal fluctuations of probe particles dispersed in swimming *Chlamydomonas* suspensions and found that their distributions of short-term displacements complied with the theoretical predictions that were made by randomly superimposing power-law-decaying fields. We discuss that the physical limit operations give rise to non-Gaussian limit fluctuations where mathematical central limiting theorem does not apply, and also give a clear-cut quantitative criterion when physical fluctuations become (non-) Gaussian. The time evolution of the distributions collapsed to a single master curve when the distributions were normalized by their standard deviations. The concept of random power-law fields explains the reason for this collapse which has been elusive so far. We also provide a qualitative explanation for the deviation from the master curve observed at the extreme tail of distributions. Heavily tailed distributions similar to those investigated in this study have been widely observed in various active systems such as living cells, *active cytoskeletons* [11,12], colloidal suspensions close to the glass transition [33], etc. Our expression was derived using the rather general assumption of random power-law fields [19]. We therefore anticipate that this theory is widely applicable to various nonequilibrium fluctuations that have been found to have heavily tailed distributions.

## ACKNOWLEDGMENTS

This work was supported by JSPS KAKENHI (Grants No. 15H01494, No. 15H03710, No. 23684036, No. 25127712, and No. 25103011), a program for improvement in research environment for young researchers in Japan.

- [1] T. G. Mason and D. A. Weitz, *Phys. Rev. Lett.* **74**, 1250 (1995).
- [2] J. Liphardt, S. Dumont, S. B. Smith, I. Tinoco, and C. Bustamante, *Science* **296**, 1832 (2002).
- [3] L. D. Landau, E. M. Lifshitz, and L. P. Pitaevski, *Statistical Physics* (Pergamon Press, Oxford, 1980).
- [4] W. Feller, *An Introduction to Probability Theory and Its Applications* (Wiley, New York, 1968).
- [5] J. Dunkel, S. Heidenreich, K. Drescher, H. H. Wensink, M. Bar, and R. E. Goldstein, *Phys. Rev. Lett.* **110**, 228102 (2013).
- [6] H. H. Wensink, J. Dunkel, S. Heidenreich, K. Drescher, R. E. Goldstein, H. Lowen, and J. M. Yeomans, *Proc. Natl. Acad. Sci. USA* **109**, 14308 (2012).
- [7] T. S. Vicsek, *Fluctuations and Scaling in Biology* (Oxford University Press, Oxford, 2001).
- [8] S. Ramaswamy, *Annu. Rev. Condens. Matter Phys.* **11**, 323 (2010).
- [9] M. C. Marchetti, J. F. Joanny, S. Ramaswamy, T. B. Liverpool, J. Prost, M. Rao, and R. A. Simha, *Rev. Mod. Phys.* **85**, 1143 (2013).
- [10] G. H. Koenderink, Z. Dogic, F. Nakamura, P. M. Bendix, F. C. MacKintosh, J. H. Hartwig, T. P. Stossel, and D. A. Weitz, *Proc. Natl. Acad. Sci. USA* **106**, 15192 (2009).
- [11] D. Mizuno, C. Tardin, C. F. Schmidt, and F. C. MacKintosh, *Science* **315**, 370 (2007).
- [12] T. Toyota, D. A. Head, C. F. Schmidt, and D. Mizuno, *Soft Matter* **7**, 3234 (2011).
- [13] D. T. N. Chen, A. W. C. Lau, L. A. Hough, M. F. Islam, M. Goulian, T. C. Lubensky, and A. G. Yodh, *Phys. Rev. Lett.* **99**, 148302 (2007).

- [14] J. L. Thiffeault, *Phys. Rev. E* **92**, 023023 (2015).
- [15] R. Jeanneret, D. O. Pushkin, V. Kantsler, and M. Polin, *Nat. Commun.* **7**, 12518 (2016).
- [16] K. C. Leptos, J. S. Guasto, J. P. Gollub, A. I. Pesci, and R. E. Goldstein, *Phys. Rev. Lett.* **103**, 198103 (2009).
- [17] I. Rushkin, V. Kantsler, and R. E. Goldstein, *Phys. Rev. Lett.* **105**, 188101 (2010).
- [18] B. V. Gnedenko and A. N. Kolmogorov, *Limit Distributions for Sums of Independent Random Variables* (Addison-Wesley, Reading, MA, 1968).
- [19] I. M. Zaid and D. Mizuno, *Phys. Rev. Lett.* **117**, 030602 (2016).
- [20] I. M. Zaid, J. Dunkel, and J. M. Yeomans, *J. R. Soc., Interface* **8**, 1314 (2011).
- [21] S. Kim and S. J. Karrila, *Microhydrodynamics: Principles and Selected Applications* (Butterworth-Heinemann, Boston, 1991).
- [22] D. Mizuno, D. A. Head, F. C. MacKintosh, and C. F. Schmidt, *Macromolecules* **41**, 7194 (2008).
- [23] M. Atakhorrami, D. Mizuno, G. H. Koenderink, T. B. Liverpool, F. C. MacKintosh, and C. F. Schmidt, *Phys. Rev. E* **77**, 061508 (2008).
- [24] K. Drescher, R. E. Goldstein, N. Michel, M. Polin, and I. Tuval, *Phys. Rev. Lett.* **105**, 168101 (2010).
- [25] J. S. Guasto, K. A. Johnson, and J. P. Gollub, *Phys. Rev. Lett.* **105**, 168102 (2010).
- [26] K. Drescher, J. Dunkel, L. H. Cisneros, S. Ganguly, and R. E. Goldstein, *Proc. Natl. Acad. Sci. USA* **108**, 10940 (2011).
- [27] T. J. Pedley and J. O. Kessler, *J. Fluid Mech.* **212**, 155 (1990).
- [28] S. Chandrasekhar, *Rev. Mod. Phys.* **15**, 1 (1943).
- [29] J. Holtzmark, *Ann. Phys. (Leipzig)* **363**, 577 (1919).
- [30] R. P. McCord, J. N. Yukich, and K. K. Bernd, *Cell Motil. Cytoskeleton* **61**, 137 (2005).
- [31] B. Wang, J. Kuo, S. C. Bae, and S. Granick, *Nat. Mater.* **11**, 481 (2012).
- [32] A. Rahman, *Phys. Rev.* **136**, A405 (1964).
- [33] E. R. Weeks and D. A. Weitz, *Chem. Phys.* **284**, 361 (2002).